CYCLOTRON WAVE INSTABILITY IN THE CORONA AND ORIGIN OF SOLAR RADIO EMISSION WITH FINE STRUCTURE

II: *Origin of 'Tadpoles'*

V. V. ZHELEZNYAKOV and E. YA. ZLOTNIK
Radiophysical Research Institute, Gorki, U.S.S.R.

(Received 24 October, 1974; in revised form 7 July, 1975)

Abstract. An interpretation is suggested of the fine structure of tadpole solar radio emission based upon the theory of Bernstein mode cyclotron instability. It is shown that the frequency spectrum of an individual tadpole is similar to the frequency behaviour of the Bernstein mode increment if the velocity of electrons trapped by the magnetic field amounts nearly to 10^9 cm s^{-1}. The absorption 'body' and emission 'tail' are associated with the instability due to the kinematic Doppler effect and the 'eye' with the instability due to the velocity dependence of the electron mass. The observed radio emission is the result of nonlinear conversion (coalescence) of Bernstein modes at different frequencies into electromagnetic waves. The appearance of separate tadpoles (interrupted character of emission in time) is attributed to the pulse injection of nonequilibrium electrons into the trap. Estimations are presented for the expected dimensions of emission region and the hot electron density necessary for Bernstein mode excitation.

1. Introduction

In Parts II and III we deal with the possibility of interpreting the elements of the fine structure of the solar radio emission such as zebra-patterns and tadpoles. An explanation of these phenomena is based on the results of investigation of the cyclotron instability of longitudinal waves in the coronal plasma (Bernstein modes and plasma waves in the hybrid band) reported in Part I (Zheleznyakov and Zlotnik, 1975). Here we draw the main attention to the dynamic spectra observed on 2 March 1970 (Slottje, 1972) (Figure 1). A special interest to this event arises from the qualitatively new phenomena in the fine structure of the solar radio emission.

The dynamic spectra of solar radio emission called zebra-pattern were first obtained by Elgarøy (1961) and then by other radio astronomers. The instantaneous frequency differences between neighbouring bands of zebra-patterns are often the same within an accuracy of the observation errors (the bands are equidistant). Nevertheless some cases are known when it is not so (see Elgarøy, 1973). The distance between the bands is of about 5 MHz. The frequency drift of equidistant or quasi-equidistant bands shows a great variety and changes even over one event. It varies in value and direction and reveals an oscillating character.

During the event on 2 March 1970 the zebra-type phenomena shows a wide range of details (Figure 1). Here the frequency distance between parallel drifting bands reaches 15 MHz. Against the background of the zebra-pattern, we can see broad-banded absorption bursts (b). A part of the dynamic spectra presented in Figure 1 testifies to the fact that sometimes the zebra phenomenon generation was of an oscil-

Solar Physics **44** (1975) 447–459.

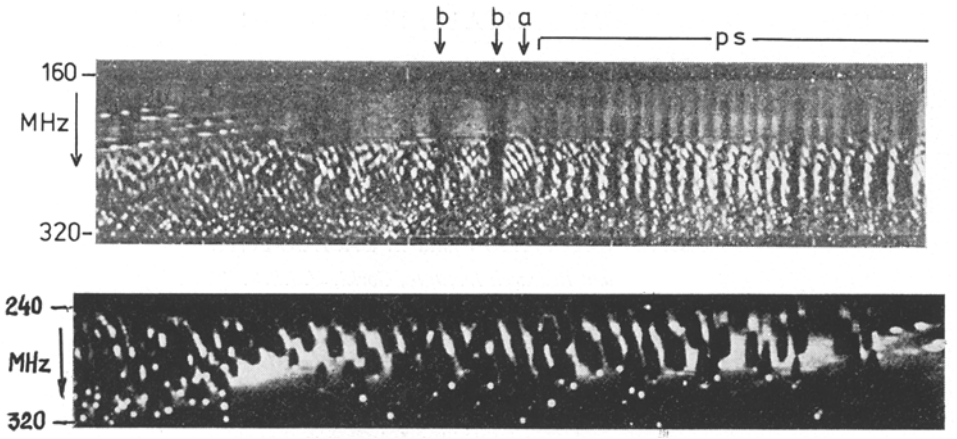

Fig. 1. Dynamic spectrum of the event on the 2 March 1970 (Slottje, 1972). Above: zebra-structure in the pulsating regime; below: tadpoles. Half-a-minute corresponds to 8×3 mm.

lating character (with the period 0.7–0.8 s). The next phase of the event on 2 March 1970 is shown in the lower part of Figure 1. The frequency intervals between neighbouring bands increased up to 40 MHz. The bands themselves dissolve into separate short-time (0.2–0.3 s) bursts, the dynamic spectra of which was like the tadpoles with a bright eye and tail. Following each other, the tadpoles have a tendency to be located on drifting parallel bands resembling a zebra and to appear at different bands simultaneously.

Such a location of tadpoles on the dynamic spectra points to the fact that they are separate elements of the zebra-structure which occur under pulsed injection of hot particles into generation region.

2. A Model of the Source

When explaining the fine structure of the solar radio emission in the event on 2 March 1970, we shall proceed from the model of a 'point' source localized in the corona at the apex of the magnetic trap (Figure 2). The dimensions of the generation region are assumed to be small enough for the inhomogeneous character of the magnetic field and the plasma density to be neglected when investigating the frequency spectrum of excited waves (see concrete requirements for the dimensions in Section 3).

The tadpole generation scheme in such a model must take into account that these elements of the fine structure are the development and continuation of zebra-structure on 2 March 1970. A specific feature is nearly equal frequency interval between the emission bands ('quasi-equidistance'). Taking into account that the tadpoles also have a tendency to be situated in such drifting bands, we conclude that both zebra and tadpole phenomena are associated with emission at the harmonics of a certain characteristic frequency. The latter is most likely the electron gyrofrequency Ω_H. It will be shown that for the 'point' source model, a possible scheme of tadpole

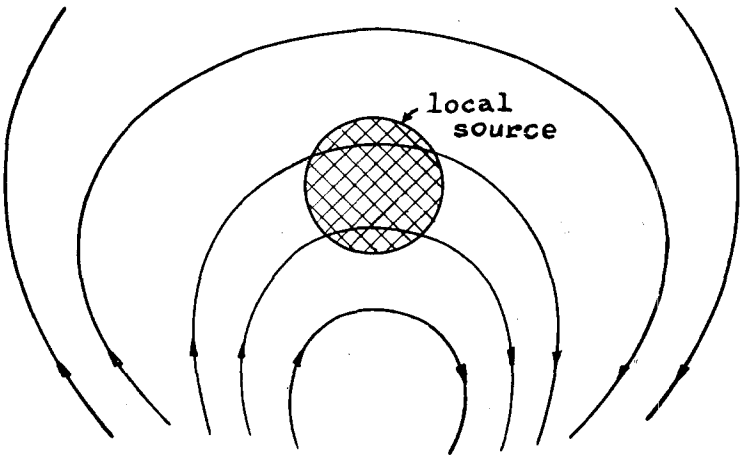

Fig. 2. Model of a point source localized at the apex of the magnetic trap.

generation which takes into account their location in the system of harmonic bands is the following. The radio emission is the result of combination scattering (coalescence) of excited Bernstein modes, corresponding to equal or different harmonics of the gyrofrequency $s_1\Omega_H$ or $s_2\Omega_H$ (s_1 and s_2 are the numbers of harmonics). The observed radio emission frequencies occupy the frequency bands

$$\omega_r \approx s_1\Omega_H + s_2\Omega_H \tag{2.1}$$

separated by the intervals $\Delta\omega \approx \Omega_H$. The frequency drift of bands in such a scheme is due to the temporal change of the frequency Ω_H, that is the magnetic field in the source. The generated radio emission escapes from the corona if $\omega_r > \Omega_p$.

The above makes it possible to estimate the expected value of the plasma frequency Ω_p and electron gyrofrequency during the tadpole period according to the dynamic spectra in Figure 1b. For the distance 40 MHz between the bands in which the tadpoles lie, $\Omega_H \sim 2\pi \times 40$ MHz (this corresponds to the magnetic field $H \sim 15$ Oe in the local source). The presence of the lower frequency boundary for zebra-tadpole emission in the event on 2 March 1970 (at about 200 MHz, see Figure 1) points to the fact that the plasma frequency Ω_p in the local source was also close to $2\pi \times 200$ MHz and did not essentially change during the whole event. Consequently, during the tadpole emission the following parameters of the local source are possible: the ratio $\Omega_p/\Omega_H \simeq 5$, the magnetic field $H \sim 15$ Oe and the plasma density 5×10^8 el cm^{-3}. The upper hybrid frequency $\Omega_h = (\Omega_p^2 + \Omega_H^2)^{1/2}$ differs slightly from Ω_p.

The frequency drift of quasi-equidistant bands of possible tadpole location $d\omega_r/dt$ cannot be related with Ω_p since $\Omega_p = \text{const}$ in the local source and the scheme (2.1) does not involve the value Ω_p. Therefore the drift is caused by the change in the magnetic field; according to (2.1),

$$\frac{d\omega_r}{dt} \approx (s_1 + s_2)\frac{d\Omega_H}{dt}. \tag{2.2}$$

From Figure 1b it follows that $d\omega_r/dt \sim 2\pi \times 70$ MHz s^{-1}. On the other hand $s_1 + s_2$ is apparently of about 6 (since $\Omega_p/\Omega_H \sim 5$). Hence during the tadpole period $d\Omega_H/dt \sim 2\pi \times 12$ MHz s^{-1}.

3. Tadpole Frequency Spectrum for Bernstein Modes

The suggested scheme provides the tadpoles to locate on the dynamic spectrum, relates tadpoles with the zebra-structure and allows to estimate coronal plasma parameters in the local source. The main problem, however, is a peculiar dynamic spectrum of each separate element (see Figure 3). It consists of the emission band at the lower frequency ('tail' with the bandwidth ~ 20 MHz) and the strong absorption interval at the higher frequencies ('body' ~ 10 MHz) terminated with a bright narrow-band dot ('eye' ~ 1–2 MHz).

When explaining the frequency structure of tadpole (or zebra), it should be taken into account that relation (2.1) is rather approximate. Indeed, the Bernstein mode frequencies are close to $s\Omega_H$ only at $\lambda \equiv k_\perp^2 v_\perp^2/\Omega_H^2 \ll s^2$ or at $\lambda \equiv k_\perp^2 v_\perp^2/\Omega_H^2 \gg s^2$. In the region $\lambda \sim s^2$ they may differ from $s\Omega_H$ up to the value Ω_H (see the dispersion curves in Part I). Therefore, the value $s\Omega_H$ in (2.1) points only to the Bernstein mode frequencies with an accuracy of the order of Ω_H. The Bernstein mode excitation is possible in a wide frequency band of the order of Ω_H. The latter is necessary for tadpole generation the total frequency width of which is comparable with the distance between drifting quasi-equidistant bands Ω_H.

Let us assume that in the tadpole generation region located in the lower corona

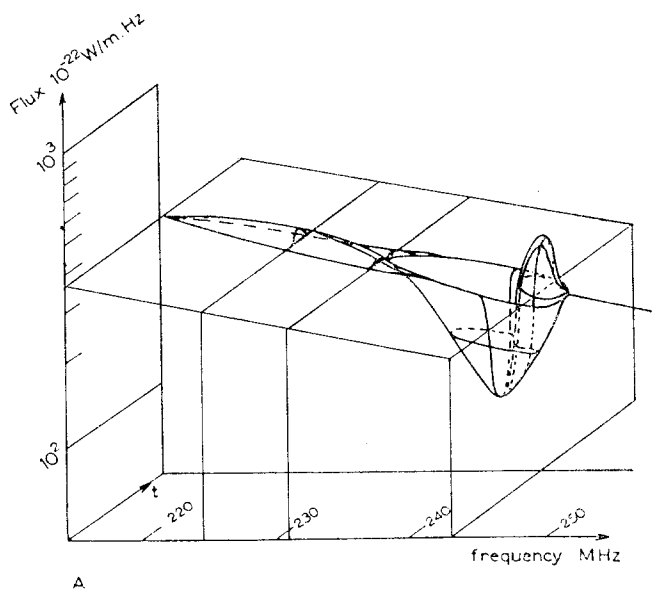

Fig. 3. Observed dynamic spectrum of a separate tadpole (Slottje, 1972).

(Figure 2) the electrons with the nonequilibrium momentum distribution of the type (I.3.3)* are embedded into the background plasma. Then, in accordance with the results of Part I, in this region there becomes possible the cyclotron instability, the kinematic and relativistic increments of which are demonstrated as a function of the frequency in Figures I.3 and I.4. It is easy to see that the kinematic increment behaviour (Figure I.3) repeats the frequency tadpole spectrum in the region emission tail-absorption body. The light emission interval corresponds to the cyclotron instability and the shadow region to the strong cyclotron absorption. A bright eye is associated with a positive relativistic increment existing in a narrow frequency band near $s\Omega_H$ (Figure I.4).

Let us find now the parameters of the non-equilibrium component which provide the characteristic values of emission and absorption bands in a tadpole. As yet, we deal with the frequency bands for Bernstein modes (longitudinal waves). The frequency spectrum of radio tadpoles will be discussed in Section 5.

The absorption bandwidth of Bernstein modes (the frequency interval occupied by the negative kinematic increment) is found from the condition inverse to the inequality (I.3.17):

$$0 < \lambda < \lambda_{cr} \approx \left(s \frac{v_T}{v_e} \right)^2 . \tag{3.1}$$

From this condition and dispersion curves in Figure I.1.b as well as directly from the plot of the frequency dependence of the kinematic increment illustrated in Figure I.3, it follows that the absorption body at the harmonic $s=2$ falls within the interval of about $0.2\Omega_H$ (at $\Omega_p/\Omega_H=5$ and $v_e/v_T=4$). For $\Omega_H \approx 2\pi \times 40$ MHz this corresponds to about 8 MHz. The bandwidth decreases with the number of s and for $s=3$ and $s=4$ it is equal to $0.1\Omega_H$.

It is also clear from Figure I.3 that within the frequency interval below the absorption band, the kinematic increment is positive. Here (in the bandwidth of about $0.8\Omega_H$ for $s=2$) the Bernstein modes are amplified that corresponds to the emission 'tail' of a tadpole.

Thus, the hot electrons with the mean velocity $v_e=4v_T$ provide the occurrence of tadpoles with the observed ratio of emission and absorption bands. The total 'length' of a tadpole ('tail'+'body') for Bernstein modes reaches Ω_H, this length being independent of the ratio v_e/v_T.

As was pointed above, the bright eye may be associated with Bernstein mode excitation due to the relativistic cyclotron instability. However the upper limit of the registered frequency band corresponding to the bright eye (1–2 MHz) is considerably wider than the theoretical value for the band $\Delta\omega$ where the relativistic increment $\gamma>0$. In the uniform magnetic field according to (I.3.29), $\Delta\omega \approx s\Omega_H v_e^2/c^2$. At the second harmonic for $v_e/v_T=4$ and $v_T/c \approx 10^{-2}$ the value $\Delta\omega \approx 3 \times 10^{-3}\Omega_H$ or about

* Here and below Roman I before the number of the figure or formula denotes the corresponding figure or formula in the paper by Zheleznyakov and Zlotnik (1975) which is cited as Part I.

0.1 MHz for the gyro-frequency 40 MHz (see also Figure I.4). The observed broadening may be caused by some inhomogeneity of the magnetic field in the generation region ($\Delta H/H$ up to 5%).

The latter implies that the maximum dimensions of the point source L do not exceed $5\times10^{-2}L_H$ where $L_H=H/(\mathrm{d}H/\mathrm{d}l)$ is the characteristic scale of the magnetic field. At $L_H\sim10^9$ cm the value $L\lesssim5\times10^7$ cm.

For Bernstein mode exitation the corresponding increment is necessary to be $\gamma>\nu_{\mathrm{ef}}$ where the collisional number ν_{ef} defines the collision damping of these waves in the background plasma. In the lower corona with the temperature $T=10^6$K and the plasma frequency $\Omega_p\sim2\pi\times200$ MHz, the value $\nu_{\mathrm{ef}}\approx35$.

The maximum kinematic and relativistic increments $\gamma_{\max}$ are determined by formulas (I.3.22) and (I.3.33), from which it follows that the value $\gamma_{\max}N_0/\Omega_HN_e$ is equal to 10^{-2} and 10^{-3}, respectively. Assuming $\Omega_H\approx8\pi\times10^7$ s^{-1} (40 MHz) and $\Omega_p\approx4\pi\times10^8$ s^{-1} ($N_0\sim5\times10^8$ cm^{-3}), we find that the kinematic cyclotron instability threshold corresponds to the hot electron density $N_e\sim7\times10^3$ el cm^{-3} and the relativistic instability threshold to $N_e\sim7\times10^4$ el cm^{-3}.

As to the correctness of these estimations, we need to say the following. In the coronal plasma apart from damping due to collisions there exists Landau damping. Its decrement γ_L in the region, defined by inequality (I.2.3), is equal to

$$\gamma_L\simeq\sqrt{\pi}\,z_Te^{-z_T^2}(\omega-s\Omega_H), \tag{3.2}$$

where $z_T=(\omega-s\Omega_H)/\sqrt{2}\,k_\parallel v_T$ (see, for example, Mikhaylovsky, 1971). Estimations show that for $v_e=4v_T$ and $\Omega_p/\Omega_H=5$ at $k_\parallel=k_\parallel^{\mathrm{opt}}$ (I.3.18) which provide the maximum kinematic increment (I.3.23), Landau damping is rather essential: γ_L exceeds ν_{ef} by three orders of magnitude. The index of the exponent in γ_L is equal to $-(v_e^2/v_T^2)\,z_s^2=-8$. Due to the latter circumstance the dependence γ_L on $k_\parallel$ turns to be rather sharp and a relative small decrease in $k_\parallel$ compared with $k_\parallel^{\mathrm{opt}}$ (more than 1.5 times) permits the inequality $\gamma_L\ll\nu_{\mathrm{ef}}$ to be fulfilled.

At the same time the change in $\gamma\sim\exp[-(\omega-s\Omega_H)^2/2k_\parallel^2v_e^2]$ where $v_e^2\gg v_T^2$ will be unessential because at $k_\parallel^{\mathrm{opt}}$ the exponent index is $-1/2$. This proves the validity of the above-made estimations of the nonequilibrium component density necessary for Bernstein mode excitation. The role of Landau damping is reduced to limitation of the interval over $k_\parallel$ in which the cyclotron instability occurs (in our model for not too large N_e, this interval $|k_\parallel|\lesssim0.7k_\parallel^{\mathrm{opt}}$).

In the region of relativistic instability, the Landau damping may be neglected since at $k_\parallel<(\omega/c)\,\beta$ (see I.3.9) the Landau decrement is smaller than the decrement due to the collision number ν_{ef}.

It is clear, however, that the hot electron density N_e at the instability threshold is yet insufficient for effective Bernstein mode amplification. It takes place only under the necessary condition

$$\mu l>1, \tag{3.3}$$

where μ is the resulting amplification coefficient related with the increment γ and decrement due to collisions ν_{ef} through the equality

$$\mu = (\gamma - \nu_{ef})\, v_{gr}^{-1} \tag{3.4}$$

(the group velocity $v_{gr} = d\omega/dk$, l is the length of a ray on which the effective amplification of the wave takes place).

In the homogeneous plasma with the constant magnetic field, l coincides with the source dimension L. In the plasma with the inhomogeneous magnetic field $l = L$ only for a small enough source ($L < L_H \Delta\alpha$; see below). The fact is that Bernstein modes are propagated and amplified only at the angle α to the magnetic field **H** close to $\pi/2$ (within the interval $\Delta\alpha \ll 1$). If the characteristic scale of the magnetic field **H** is L_H, the length of the ray $l \approx L_H \Delta\alpha$. In particular, for the kinematic cyclotron instability at $s = 2$ and $\Omega_p/\Omega_H = 5$, the interval $(\Delta\alpha)^{kin} \sim 0.15$. This interval is obtained from the dispersion curves in Figure I.1b and formula (I.3.18) with taking into account the above remarks on shortening the instability interval over $k_\parallel$.

For the relativistic cyclotron instability at the frequencies, corresponding to the maximum increment, the interval of angles is considerably less: $(\Delta\alpha)^{rel} \sim 4 \times 10^{-2}$. To find this value, the formula (I.3.9) and dispersion equation (I.2.6) were used.

Further, assuming $L_H \sim 10^9$ cm for the model of the local source in the corona, we find the length l on which the effective amplification of the given Bernstein mode occurs. For the kinematic instability $l \sim 1.5 \times 10^8$ cm and for the relativistic instability $l \sim 4 \times 10^7$ cm. For such values the condition $\mu l > 1$ (3.3) may be easily satisfied when N_e is just above the instability threshold (by 3×10^3 el cm^{-3} for the kinematic instability and by 5×10^4 el cm^{-3} for the relativistic instability).

Certainly, these preliminary estimations do not determine the hot electron density in the source which is enough to generate the radio emission of the observed intensity. It is possible to answer this question only using the nonlinear theory of Bernstein mode excitation and their conversion into electromagnetic radiation.

4. Time Behaviour

We emphasized several times the evident fact that for the appearance of separate tadpoles not merged into continuous bands, there is needed the pulse injection of hot particles into the generation region with duration less than the lifetime of a tadpole (<0.1–0.3 sec). On the whole, the conditions and the character of injection are the subject of special research. Note only that we may imagine injection as compression of the region occupied by energetic nonequilibrium particles up to the dimensions necessary for the effective longitudinal wave excitation or as a fast acceleration (heating) of a part of coronal particles up to the needed energies (within the generation region itself, without transporting from outside).

As observations show, the formation of the radiation source develops in such a way that the generation of a tadpole 'body' and 'tail' begins earlier than that of the eye. It is due to the fact that an eye is caused by the relativistic instability for which

$\gamma > \nu_{ef}$ is realized at the higher electron density of the nonequilibrium component N_e than for kinematic instability (see Section 3).

It may be assumed that the radio emission of a tadpole ceases due to decay of the nonequilibrium distribution function during quasi-linear relaxation associated with the relativistic instability. The characteristic time of this relaxation $\tau \sim 1/\gamma \ll 1/\nu_{ef}$ (if $\gamma \gg \nu_{ef}$) and the duration of an 'eye' is determined then by the damping time $\tau^{coll} \simeq 1/\nu_{ef}$ of excited plasma waves (Bernstein modes). Since in the tadpole generation region at $T \sim 10^6$K, $\nu_{ef} \simeq 35$, the damping time $\tau^{coll} \sim 3 \times 10^{-2}$ s. With some increase in the temperature T, the damping time $\tau^{coll} \sim T^{3/2}$ is comparable with the observed lifetime of an eye (0.1 s). It may happen also that the lifetime of a tadpole is determined by the diffusion time of particles from the source. For the source dimensions $L \sim 10^8$ cm and the particle velocity $v_e \simeq 4v_T \simeq 10^9$ cm s^{-1}, the time $t \sim L/v_e \sim 0.1$ s.

Certainly, the appearance of a black absorption body on Bernstein modes is impossible without a continuous excitation of these modes ('light background'; see Figure 1b) by some agent acting for a long time. Such an agent may be the energetic electrons with the momentum distribution of (I.3.3)-type, injected all the time into the tadpole generation region. If the parameter v_e/v_T exceeds the corresponding value $v_e/v_T \sim 4$ inherent in the electrons responsible for the tadpole generation due to the kinematic cyclotron instability of Bernstein modes, there will be the background with the enhanced energy density W_s^b at those frequencies which correspond to the negative increment in the tadpoles. Then, with the pulse injection of nonequilibrium electrons with $v_e/v_T \sim 4$, the energy density of Bernstein modes decreases sharply in the frequency band where the increment is negative and increases compared with W_s^b in the region of the positive increment.

5. Conversion into Electromagnetic Radiation

We have considered above the tadpole generation on Bernstein modes (longitudinal waves). However these elements of the fine structure are recorded on the dynamic spectrum of radio emission (transverse waves). Therefore it is necessary to discuss the nonlinear conversion processes which transform a tadpole on Bernstein modes into that on the electromagnetic waves. Such a process may be the combination scattering (coalescence) of two Bernstein modes into the electromagnetic radiation. A detailed investigation of such a process is not yet completed. Therefore we confine ourselves only to some remarks.

For the coalescence of Bernstein modes with the harmonic numbers s_1 and s_2, the conservation laws

$$\omega_1 + \omega_2 = \omega_r, \tag{5.1}$$

$$\mathbf{k}_1 + \mathbf{k}_2 = \mathbf{k}_r, \tag{5.2}$$

are to be satisfied. Here $\omega_1 = s_1\Omega_H$, $\omega_2 = s_2\Omega_H$ and $\mathbf{k}_1$, $\mathbf{k}_2$ are the frequencies and the wave vectors of Bernstein modes, ω_r and $\mathbf{k}_r$ are the frequency and the wave vector of

a radio wave. The value $\mathbf{k}_r = (\omega_r/c)\, n$ (n is the refractive index). Assuming $\omega_r = \omega_1 + \omega_2 \approx (s_1 + s_2)\, \Omega_H$ and taking into account that $n < 1$, we estimate $k_r < \Omega_H (s_1 + s_2)/c$. For Bernstein modes propagating almost across the magnetic field, $k_{1,2} \approx k_{\perp 1,2} \equiv \equiv \sqrt{\lambda_{1,2}}\, \Omega_H / v_T$ (see designations to the formula (I.2.2)). Then obviously $k_r \ll k_{1,2}$ if $\lambda \gg (s_1 + s_2)^2 v_T^2/c^2$. In the tadpole generation region $v_T/c \sim 10^{-2}$ and $s_1 + s_2 \sim 5$–6. Therefore the condition $k_r \ll k_{1,2}$ will be correct within a wide interval of the values of λ satisfying the inequality $\lambda \gg 3 \times 10^{-3}$. Using the plots in Figure I.3b and I.4, the dispersion curves of Figure I.1b as well as the dispersion dependence for Bernstein modes (I.2.6), it may be seen that the inequality $\lambda \gg 3 \times 10^{-3}$ is satisfied for the region of the kinematic instability and absorption and for the maximum of the relativistic instability at the harmonics $s = 3$–5, as well as for a considerable part of the instability interval at the harmonic $s = 2$.

Due to inequality $k_r \ll k_{1,2}$ the combination scattering of Bernstein modes occurs on opposite waves: $\mathbf{k}_1 \approx -\mathbf{k}_2$ (see (5.2)). The latter permits the conservation law (5.2) to be easily satisfied for any given direction of the radio emission in the source. Due to this in simultaneous registration of the eye and tail of a tadpole, it becomes unessential that relativistic and kinematic instabilities of Bernstein modes are realized at close to $\pi/2$ but different angles α to the magnetic field $\mathbf{H}$.

Then, the ratio $\mathbf{k}_1 = -\mathbf{k}_2$ testifies to the closeness of the values of the parameter $\lambda = k_\perp^2 v_T^2/\Omega_H^2$ for both coalescing Bernstein modes. From this it follows that at $s_1 = s_2$ the waves, excited in the relativistic instability region, are scattered on the waves of the same region. This is valid both for the kinematic instability region and the kinematic absorption region.

The coalescence of Bernstein modes with the energy density W_s gives rise to the radio emission with the intensity $I(\omega_r)$ proportional to W_s^2. It is true if W_s is not too great and the inverse process of decaying the electromagnetic waves into Bernstein modes is unessential. For large W_s the decay leads to the fact that the effective temperature of radio emission T_r reaches the effective temperature $T_s \sim W_s(\omega)$ of excited Bernstein modes. In these cases the frequency spectrum $I(\omega_r)$ repeats the frequency spectrum $W_s^2(\omega)$ or $W_s(\omega)$ respectively, and coincides qualitatively with the observed one.

The frequency spectrum of a tadpole in the radio emission may be explained in such a way. If the energy density of excited Bernstein modes W_1 and W_2 are not too great, the decay (process inverse to coalescence) influence on the intensity of generated radio emission $I(\omega_r)$ will be unessential. In this case

$$I(\omega_r) = A W_1(\omega_1)\, W_2(\omega_2), \tag{5.3}$$

where $\omega_r = \omega_1 + \omega_2$, the frequencies $\omega_1 = \omega_1(\mathbf{k}_1)$ and $\omega_2 = \omega_2(\mathbf{k}_2)$ $\mathbf{k}_1 \simeq -\mathbf{k}_2$. The factor A is the function of ω_1, ω_2, $\mathbf{k}_1$ and $\mathbf{k}_2$. Its finding is just one of the main problems of the nonlinear conversion. We assume for rough estimations that $A = \text{const}$ and the energy densities W_1 and W_2 repeat qualitatively the increment behaviour $\gamma(\lambda)$ at the corresponding harmonics (in Figure 4a such dependences are given for the harmonics $s_1 = 2$ and $s_2 = 4$). Then the frequency spectrum of a tadpole (5.3) without

'eye', plotted with allowance for the dispersion curves of Figure I.1b, takes the form illustrated in Figure 4b.

It is seen from Figure 4b that the whole extension of a 'tadpole' in radio waves increases and reaches $2\Omega_H$ (but not Ω_H as for Bernstein modes). Since the tadpoles with various numbers of the harmonics s_1 and s_2 are frequency-shifted by the value Ω_H, $2\Omega_H$, $3\Omega_H$ etc, the given circumstance leads to overlapping of separate elements of the structure. Such overlapping is well seen on the dynamic spectrum in Figure 1b.

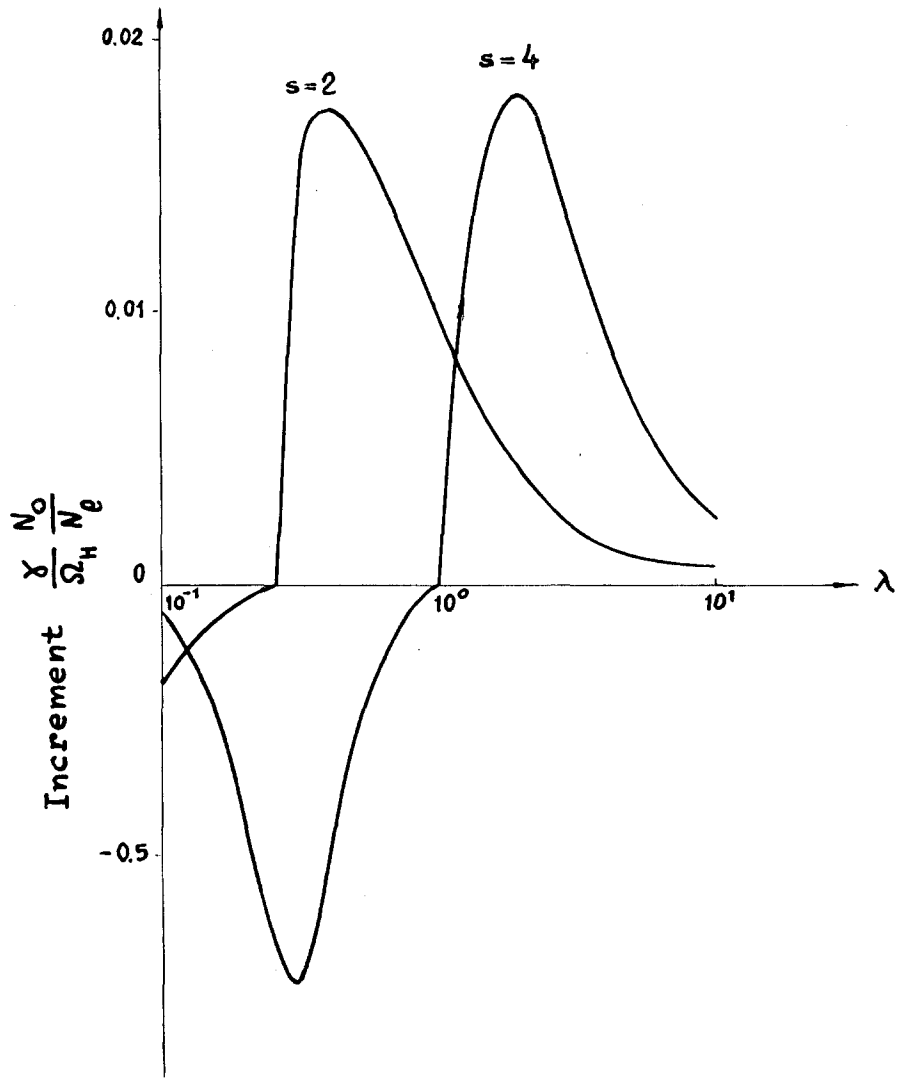

Fig. 4a.

Fig. 4. Computed frequency spectrum of a separate tadpole without 'eye'. (a) dependence of the kinematic increment on λ at $s_1=2$ and $s_2=4$, $v_e=4v_T$; (b) qualitative dependence of W_1W_2 on the frequency.

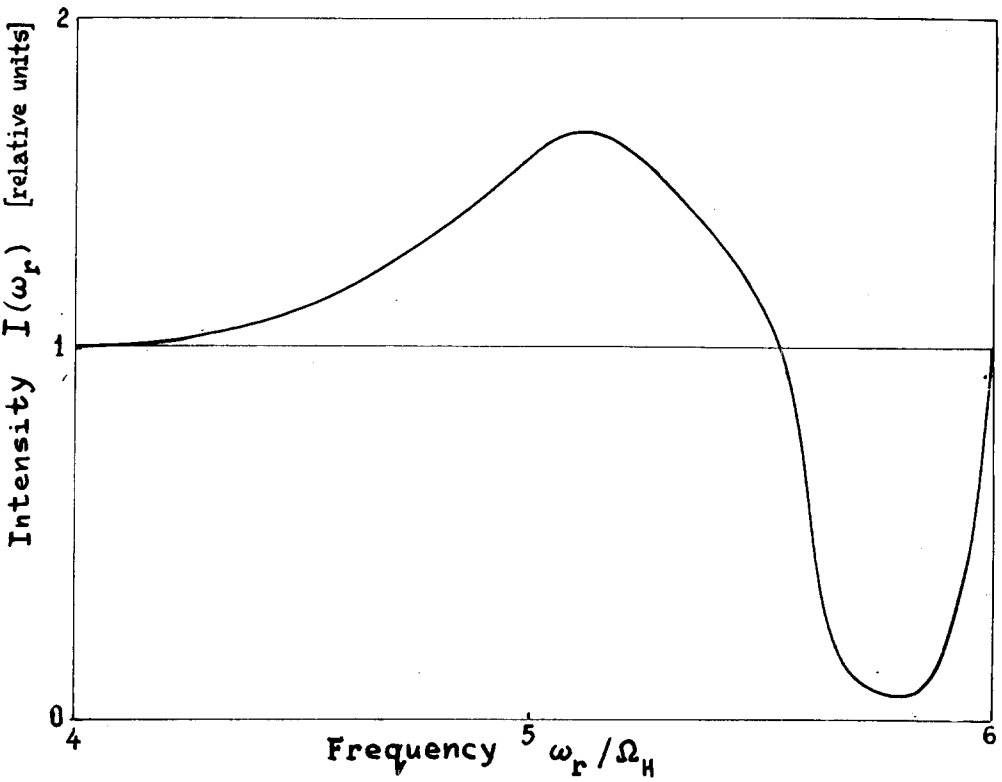

Fig. 4b.

6. Variations of Tadpole Form

In a large number of cases (also during the event of 2 March 1970 and earlier, for example, in observations made by Elgarøy (1961)) there were recorded separate bright dots ('eyes', 'knots') on the dynamic spectra. The absence of a tadpole itself (body and tail) might be associated with its lower intensity as compared with that produced by the relativistic increment. The higher values of the latter will be provided if the energetic electrons have the momentum distribution with the greater derivative $df/\partial p_\perp$ than that of (I.3.3).

The second possibility of isolated dot appearance on the dynamic spectrum is connected with injection of more energetic (than it is necessary for the developed tadpole generation) electrons into the local source. In this case a tadpole is compressed up to the dimensions of the frequency interval typical of the relativistic cyclotron instability.

It may be emphasized that a masking effect of the relativistic instability occurs at the smaller values of the parameter v_e/v_T, when s is large. There may be the situation when both relativistic and kinematic instabilities are essential at the lower harmonics (providing for instance, the interrupted zebra-pattern generation). Simultaneously at the higher harmonics and higher frequencies, essential is only the relativistic in-

crement which gives rise to bright 'knots' on the dynamic spectrum. It is just the case which is possibly observed on the dynamic spectrum of Figure 1a.

On the contrary, the appearance of tadpoles without eyes may be accounted for the smaller values of the relativistic increment than of the kinematic one. With the energetic electron density being insufficiently higher, the kinematic instability is realized under the conditions when for the relativistic instability the threshold density is not yet achieved (cf. formulas (I.3.23) and (I.3.33)).

During the event on 2 March 1970 the cases were noted when the tadpoles had no emission tail or were only observed in absorption. The absence of emission and the presence of the intense absorption body may be attributed to the peculiarities of the frequency behaviour of the kinematic increment the modulus of which in the absorption band is by the order of magnitude higher than in the instability band (see Figure I.3). Due to this there may be a situation when the energetic electron density is sufficient to produce a strong absorption in the tadpole body but insufficient to generate the emission tail.

7. Conclusion

In conclusion it should be noted that the suggested scheme of generation (excitation of the cyclotron instability of Bernstein modes by weakly relativistic electrons with subsequent coalescence of these modes into the electromagnetic radiation) permits the features of elements of the fine structure such as tadpoles to be explained. The main section is certainly an explanation of the frequency spectrum of a separate tadpole.

The principal point in interpreting the observed frequency spectrum is the possibility of realizing simultaneously the relativistic and kinematic cyclotron instabilities for waves with anomalous dispersion. Such a peculiarity is inherent in Bernstein modes at the frequencies below the hybrid frequency and just therefore they were used to give account for the tadpole fine structure.

Finally let us mention another possibility to interpret the tadpole-type spectrum in the framework of the cyclotron instability on Bernstein modes. It is connected with a large increase in the band of the relativistic decrement as far as the energy of non-equilibrium electrons increases. In accordance with (I.3.29) the frequency interval of the relativistic instability is $\Delta\omega \sim s\beta^2$. As is seen from Figure I.4, the relativistic absorption band is at least by the order of magnitude wider. For $s=3$ and $\beta \approx 0.2$ the region of relativistic absorption occupies $\sim 0.1\Omega_H$. The kinematic instability region is also broadened with β and at $\beta \approx 0.2$ covers almost all the interval Ω_H. Under such conditions the eye may be associated as before with the relativistic instability and the tail with a part of the kinematic one. A new moment here is the explanation of the 'absorption body' by the presence of a wide frequency band of the relativistic decrement within the small limits of the angles α near $\pi/2$. The level of longitudinal waves excited outside this angle interval but just at the same frequencies is small enough due to shortening of the ray path l on which the waves are amplified. This effect is caused by the absorbing 'border' at $\alpha=\pi/2$ (in the inhomogeneous magnetic field) which is met by the waves excited in the kinematic instability region. The last version

of the origin of tadpoles has to be carefully examined. When interpreting the event on 2 March 1970 in Part II, however, we prefer the first version. This is due to the fact that the presence of fast electrons with $\beta \approx 0.2$ in the source may result in the pulsating regime of tadpole generation (see, in detail, Part III). Such a regime was apparently absent during tadpole generation on 2 March 1970.

References

Elgarøy, Ø.: 1961, *Astrophys. Norv.* **7**, 123.
Elgarøy, Ø.: 1973, *Proceedings of the Third Meeting of the CESRA,* 1972 (Floriac), p. 170.
Mikhaylovsky, A. B.: 1971, *The Theory of Plasma Instabilities,* vol. I, Atomizdat, Moscow.
Slottje, C.: 1972, *Solar Phys.* **25**, 210.
Zheleznyakov, V. V. and Zlotnik, E. Ya.: 1975, *Solar Phys.* **43**, 431 (Part I).
Zheleznyakov, V. V. and Zlotnik, E. Ya.: 1975, *Solar Phys.*, this issue, p. 461 (Part III).